International Journal of Engineering Trends and Technology
ISSN: 2231–5381 / https://doi.org/10.14445/22315381/IJETT-V71I7P227

Volume 71 Issue 7, 279-289, July 2023

Original Article

Robust Digital Image Watermarking using Artificial Bee Colony Optimization with Dual-Tree Complex Wavelet Transform based SVD Approach

R. Parthiban[1], S. Manikandan[2]

[1]*Department of Computer Science, Government Arts and Science College, Kovilpatti, Thoothukudi, India.*
[2]*PG Department of Computer Science, Government Arts College, Chidambaram, India.*

[1]*Corresponding Author : parthiban.r68@gmail.com*

Received: 08 April 2023 Revised: 17 June 2023 Accepted: 21 June 2023 Published: 21 July 2023

Abstract *- Digital Image Watermarking (DIW) can be defined as the process of inserting a watermark or digital sign into digital images to protect them from unlawful use and for copyright protection. This method transforms the original image into watermarked images that have unique and watermarking imageries. The watermark must be robust to image processing attacks like cropping, compression, and resizing while protecting the visual qualities of a watermarked image. The core objective of DIW is to grant a secure and potential manner of ownership protection and authenticity of digitalized images in the modern era. This study develops a new Artificial Bee Colony Optimization with Dual-Tree Complex Wavelet Transform based SVD (ABC-DTCWT-SVD) approach for DIW. The primary objective of the ABC-DTCWT-SVD technique is to develop an image watermarking system to satisfy the requirements of imperceptibility and robustness. In the ABC-DTCWT-SVD technique, the watermarking is embedded in the DWT subband's singular value. The watermarking will not be embedded straightaway on the wavelet coefficient but rather on the components of singular values of the cover imageries' DWT subband. In addition, the ABC algorithm is used for the parameter tuning of the SVD approach and thereby maximizes the Peak Signal-to-Noise Ratio (PSNR) values. The experimental analysis of the ABC-DTCWT-SVD approach stated its promising performance over other techniques.*

Keywords *- Digital image watermarking, Embedding process, Artificial bee colony, Wavelet transform, Security.*

1. Introduction

Digital watermarking has grabbed a lot of attention and has several applications, which include secret communication, copyright protection, measurement, and authentication. DIW has protected content by inserting a signal, imperceptible data (i.e., copyright protection data) into the host image without an obvious degradation in visual quality [1]. Subsequently, watermarked images can be marked and developed as public or transferred to users [2]. Detected or Extracted watermarks are typically for content authentication and copyright protection. Scientists interested in DIW encounter difficulties in making novel techniques with suitable requirements (to serve their projected applications) [3]. The vital necessities for any watermarking method include capacity, robustness, security, and imperceptibility [4].

As per the domain where the watermark is inserted [23], such methods are divided into 2 categories they are transform, and spatial domain approaches [6]. Inserting the watermarking into the spatial element of the actual Imagery was a direct approach. It includes the merits of easy implementation and low complexities. Yet, the spatial-domain approaches were usually fragile towards image processing functions or other outbreaks [7] [8]. Some of the instances of wavelet transforms are redundant DWT (RDWT), Discrete wavelet transform (DWT), integer wavelet transforms (IWT), and redistributed invariant discrete wavelet Transform (RIDWT) [9]. Most image watermarking methods enhance their performance by integrating two or more transforms; these techniques are referred to as hybrid methods. This concept depends on the assumption that integrating more transforms can make up for defects of an individual transform, resulting in a potential technique [10].

This study develops a new Artificial Bee Colony Optimization with Dual-Tree Complex Wavelet transform-based SVD (ABC-DTCWT-SVD) approach for DIW. In the ABC-DTCWT-SVD technique, the watermarking is embedded in the DWT subband's singular value. The watermarking will not be embedded straightaway on the

wavelet coefficient but rather on the components of singular values of the cover imageries' DWT subband. In addition, the ABC algorithm is used for the parameter tuning of the SVD approach and thereby maximizes the Peak Signal-to-Noise Ratio (PSNR) values. The result analysis of the ABC-DTCWT-SVD approach stated its promising performance over other techniques.

2. Related Works

El-Kenawy et al. [11] devised an innovative technique for DIW that uses dipper-throated optimization (DTO), discrete cosine transforms (DCT), stochastic fractal search (SFS), and DWT algorithms. This method includes calculating the DWT on the cover imageries to extract its sub-elements. A discrete cosine transform (DCT) was performed to change these sub-elements into the frequency domain. The authors utilized an advanced optimizer technique called DTOSFS to determine the optimal 2 parameters: the embedding and coefficient scaling factor used while embedding a watermark into cover images. In [12], a technique for DIW was modelled. This technique depends on Singular Value Decomposition (SVD), Graph-based Transform (GBT), and DWT, which utilizes a WOA for identifying the optimal values for inserting parameters. Utilizing the GBT and DWT, the cover images were first converted. Then watermark logo was entrenched in the cover imageries' singular values.

In [24], the ultimate aim is to grant security and authentication to aerial RS imageries sent online by this hybrid technique utilizing both the SVD schemes and Redundant DWT (RDWT) for DIW. SVD and 1-level RDWT were also implemented on digitalized cover images, and a singular matrix of HL and LH subbands has opted for embedding a watermark. Also, to attain high-quality DIW results, a fusion Grasshopper–BAT (G-BAT) SC-based optimizer technique was devised, and a comprehensive comparative study against other techniques was offered. In [14], SVD based DIW method was modelled in hybrid DWT and DCT utilizing optimizer techniques like the Jaya algorithm and PSO. The watermark images (WIs) are entrenched into the lower frequency DWT subband of DCT of cover images. Jaya algorithms and PSO were implemented to enrich the quality and security threats by evaluating the fitness function.

In [15], the optimized DWT was used to embed the watermark. The optimizer algorithm was an amalgamation of the Tunicate Swarm Algorithm (TSA) and Simulated Annealing (SA). After executing the embedding procedure, the extraction was processed by RNN-based LSTM. From the extracting procedure, the unique Imagery can be attained by this abovementioned approach. Pourhadi and Mahdavi-Nasab [25] presented an optimized robust DIW approach that depends on Stationary Wavelet Transform (SWT) with the use of Speed-Up Robust Features (SURFs) and Bat Optimization Algorithm (BA). This technique enforces a higher frequency coefficient of SWT of host imagery in BA structure for optimizing watermarking strength components in the embed procedure, considered appropriate outbreaks. At last, the SURF detectors are used on the watermarked images to receive point features.

3. The Proposed Model

This research has introduced a new ABC-DTCWT-SVD approach for DIW. The primary objective of the ABC-DTCWT-SVD technique is to develop an image watermarking system to satisfy the requirements of imperceptibility and robustness. In the ABC-DTCWT-SVD technique, the watermarking is in its embedding form in the cover imageries' singular value DWT subbands. The watermarking will not be straightaway embedded on the wavelet co-efficient but rather on the components of the singular value of the cover imageries' DWT subbands.

3.1. Overview of the DTCWT Model

The concept of 1D- DWT and its enforcement by subband code is expanded to 2D- DWT for digitalized imageries [17]. In subband image recognition, the abstraction of approximate form in vertical and horizontal directions was needed. Thus, the image analysis needs $2D$ filter by multiplying wavelet and scaling functions in both directions, as follows.

$$\phi(m1, \mathrm{m2}) = \phi(m1)\phi(\mathrm{m2}) \quad (1)$$

$$y^{H}(m1, \mathrm{m2}) = \psi(\mathrm{m1})\phi(\mathrm{m2}) \quad (2)$$

$$y^{V}(m1, m2) = \phi(m1)\psi(m2) \quad (3)$$

$$y^{D}(m1, m2) = \psi(m1)\psi(m2) \quad (4)$$

From the expression, ϕ characterizes the approximate, ψ^{∇} vertical, ψ^{H} horizontal and ψ^{D} diagonal details correspondingly. LL, HL, HH and LH frequency subbands can be obtained at each decomposition level. The overall amount of DWT coefficients in every subband always remains unchanged as the overall amount of pixels in an image. Then, the decomposition of images is performed on the LL subband that provides DWT coefficients. Further, when decomposition is done, three will be a loss of resolution in the recently generated subbands. Therefore, DWT has perfect reconstruction. However, shift dependence and poor directional selectivity.

The solution to the issue was DTCWT, a type of DWT that generate a complex coefficient through a DWT filter with a complex-valued wavelet and scaling function that applies 2 real DWT was initially developed by Kingsbury in 1998. DTCWT has a duplication factor of $2D$ that can be lesser than DWT. The DTCWT provides 3 sub-imageries in every

spectral quadrant having 6 band pass sub-imagery of convolutional coefficient.

$$\psi_c(t) = \psi_r(t) + j\psi_j(t) \quad (5)$$

In Eq. (5) $\psi_r(t)$ denotes the wavelet and real co-efficient and $\psi_j(t)$ indicates imaginary and odd wavelet coefficients are formulated by:

$$(j,n) = (j,n)[jd_i + d_r] \quad (6)$$

$$|d_c(j,n)| = \sqrt{[\{d_r + d_i\}(j,n)]^2} \quad (7)$$

$$\angle d_c(j,n) = \arctan\left(\frac{d_i}{d_r}[j,n]\right) when\ |d_c(j,n)| > 0 \quad (8)$$

The size of the convolutional co-efficient (7) shows the existence of singularity, and (8) provides its location. Figure 1 demonstrates the construction of the DTCWT method.

3.2. SVD Model

The SVD is a complex or real matrices factorization in linear algebras [18]. For $m \times n$ matrix that is really complex or singular value decomposition $A = U\Sigma V$, where U denotes an $n \times n$ unitary matrix, Σ indicates an $m \times n$ rectangular diagonal matrix having a singular value of A, and V shows the $m \times m$ complex or real unitary matrix. SVD must factorize the matrix and should not be of full rank, and sigma was not smaller). SVD is suited in wavelet fields because of the homogenous region in an image. In SVD singular value represents the intensity data regarding the image; by altering the singular value, one could attain an image with a better appearance.

3.3. Optimal ABC-based SVD Approach

The ABC algorithm is used for the parameter tuning of the SVD approach and thereby maximizes the PSNR values. The ABC comprises scout, employed and onlooker bees. Each bee is presently using food sourcing [19]. The utilized bee exploits the food sources, which carries the data with respect to the food sources back to the hive and shares the data with employed bees. Onlooker bees will wait in the hive for the data to be shared through the employed bee regarding their food sources discovered, and scouts' bees will often search for the newest food source nearby the hive. Employed bee shares data regarding food source by dancing in the selected region inside the hive. The onlooker bee watches the dance and selects a food source. Every time a food source is extensively used, employed bees related to it abandon the food source and become scouts. Scout bees allow us to visualize the task performed by the exploration, while onlooker and employed bees allow us to visualize the task performed by the exploitation.

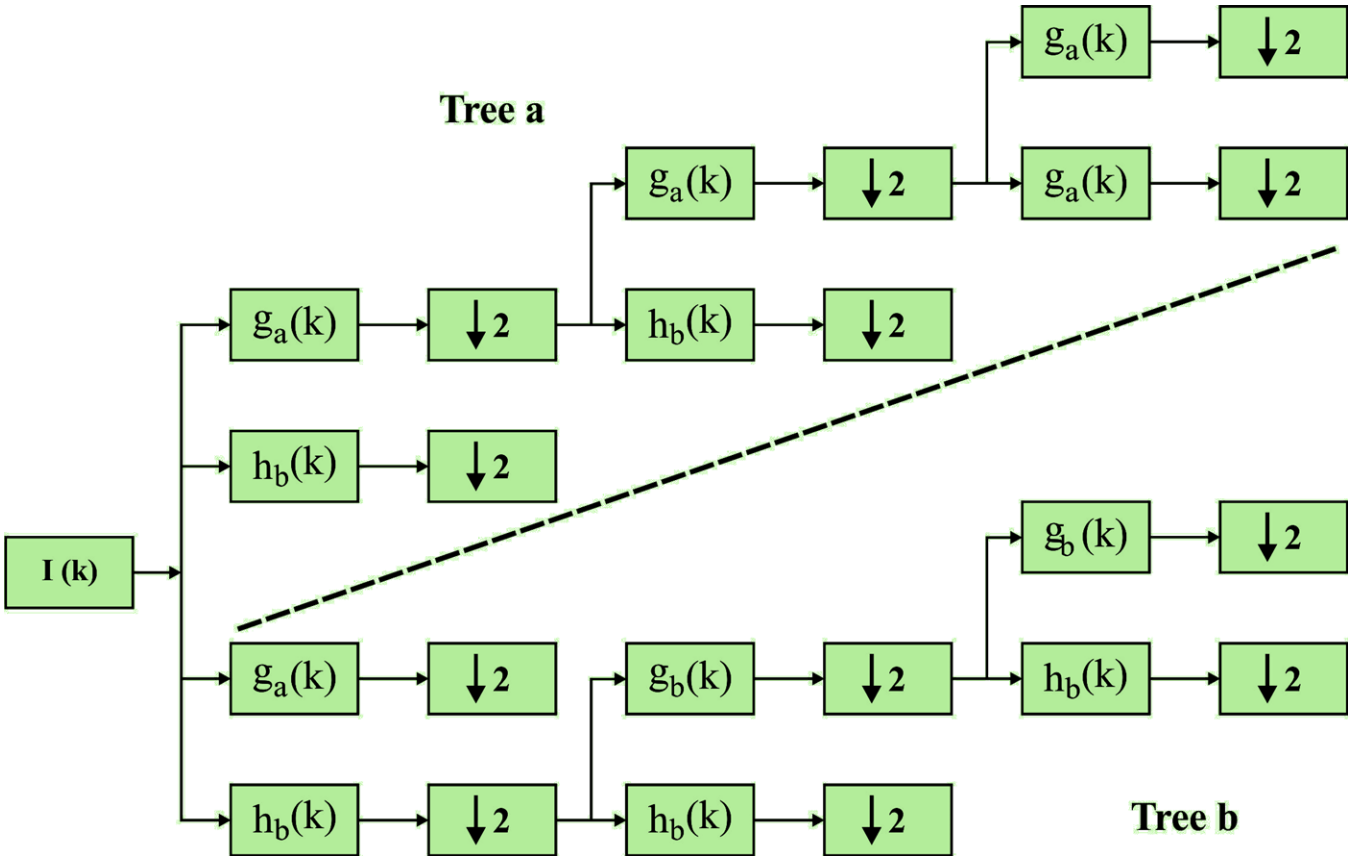

Fig. 1 Construction of the DTCWT method

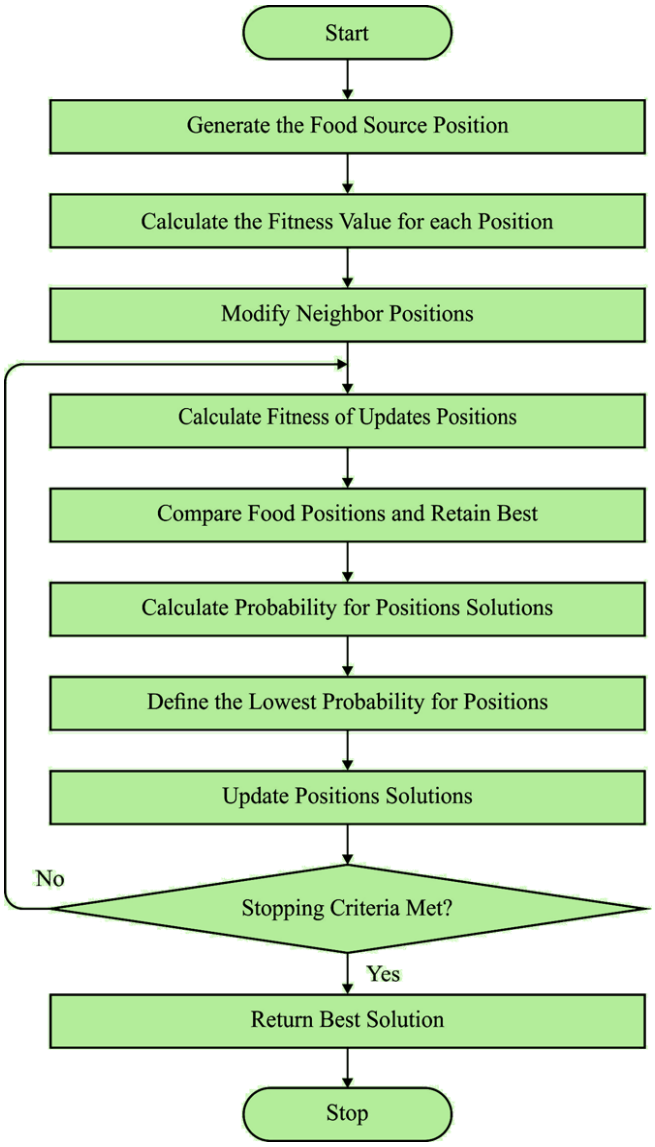

Fig. 2 Flowchart of ABC technique

In this work, every food source was a potential solution for the given issue, and the nectar quantity of food sources signifies the quality of the solution characterized by the fitness value. The quantity of food sources can be similar to the amount of employed bees, and there was accurately just a single employed bee for all the food sources.

Based on the P_i probability value, the onlooker bee chooses the food sources related to that food source,

$$P_i = \sum_{i=1}^{\frac{fir_i}{SN}} fit_i \tag{9}$$

In Eq. (9), fit_i denotes the fitness value of ith solution,· SN shows the food sourcing amount that is equivalent to the amount of onlookers or employed bees.

To generate a candidate food location $V_i = (v_{[i,1]}, v_{[i,2]}, \dots, v_{[i,G]})$ from the older one $X_i = (x_{[i,1]}, x_{[i,2]}, \dots, x_{[i,G]})$ in memory, the ABC applies the subsequent formula:

$$v_{i,j} = \Phi_{i,j}(x_{i,j} - x_{k,j}) + x_{i,j} \tag{10}$$

Whereas $k \in \{1,2,3,4 \dots, SN\}$ and $j \in \{1,2,3,4 \dots, G\}$ denotes the randomly selected index; k should be different from i,· G indicates the amount of parameter; $\Phi_{i,j}$ denotes the randomly generated value within $[-1,1]$. Figure 2 defines the ABC approach's flowchart.

Once every location of the candidate source is generated and assessed by the artificial bee, its activity is compared to the older one. If the newest food source has better or equivalent quality compared to the older source, then the older one can be replaced with the newest one. Then, the older one is retained. If a location could not be further enhanced by the predefined amount of cycles, then the food sources are considered abandoned. The predefined cycle numbers are a control parameter of the proposed model. Given that the abandoned sources are X_i and j $\in \{1,2, \dots, G\}$, then the scout discover novel food sources to be replaced by X_i as follows

$$\chi_{i,j} = \chi_{\min,j} + rand(0,1)(x_{\max,j} - x_{\min,j}). \tag{11}$$

The ABC algorithm derives a fitness function with the maximization of PSNR. It can be represented as follows.

$$fitness = \max\{PSNR\} \tag{12}$$

3.4. Watermark Embedding and Extraction Process

The frames are divided into the U, V, Y channels, and due to their better perceptibility, the U channel is selected as an embedding location [20]. The three-stage DTCWT transformed to (a) decompose U into 6 higher pass subbands and 1 low pass subband. Every subband is related to various directions. The SVD conversion was performed on every high-pass subband correspondingly. The singular values of the high pass subband as candidate coefficient are represented as $SV_d^{i,d}$. The candidate coefficient was evaluated as follows.

$$U_d^{i,k}(SV_d^{i,k})V_d^{i,k^T} = SVD(U_{3,d}^{H,k}) \tag{13}$$

The frames are divided into the U, V, Y channels, and due to their better perceptibility, the U channel is selected as an embedding location. The three-stage DTCWT transformed to (a) decompose U into 6 higher pass subbands and 1 low pass subband. Every subband is related to various directions. Assume a video with k framing, the huge pass subband in the kth framing afterwards, DTCWT decomposition is represented as $U_{l,d}^{H,k}$. The low pass subband is represented as U^L, and SVD conversion was performed on every high-pass subband correspondingly. The singular values of the high pass subband as candidate coefficient are represented as

$SV_d^{\mathrm{i,d}}$. The candidate coefficient was evaluated as follows.

$$U_d^{i,k}\left(SV_d^{i,k}\right)V_d^{i,k^T} = SVD\left(U_{3,\mathrm{d}}^{H,k}\right) \tag{14}$$

3.4.1. Watermark Embedding Process

The 6 candidate coefficients for all the frames are represented as $SV_1^{i,k}, SV_2^{i,k}, SV_3^{i,k}, SV_4^{i,k}, SV_5^{i,k}, SV_6^{i,k}$. The curve shape made from 6 candidate co-efficient beforehand (b) embedding a watermarking is *W*"-shaped, with Subband 1 and 4 at the bottom. The embedding of the watermark was performed by altering the curve shape. Initially, the curve made from the candidate co-efficient of unique frames is represented by $m(\mathrm{d}, y): y = m(d)$, in which d signifies the amount of high-pass subbands and y signifies the singular value.

Assume a binary watermark bit $Error::0x0000$ whose values are equivalent to -1/1, the embedding of the watermark was conducted by altering the general tendency of the curve. The curve as a monotonically decreasing or increasing line was remodeled. According to Eq. (15), the candidate coefficient can be modified:

$$\begin{cases}\widehat{m}: y = y_0 + k\{x - x_0\}\,(w = 1)\\ \widehat{m}: y = y_0 + -k\{x - x_0\}\,(w = -1)\end{cases} \tag{15}$$

Where χ_0 and y_0 indicates x and y values of the points $m(0,0)$, x signifies the amount of huge-pass subband, and y characterizes the singular value, k signifies embedding strength whose parameter is larger than zero. The dimension of k is a tradeoff between the quality of robust and visual. It is noted that the common trend of the curve is kept afterwards, implementing the inverse DTCWT.

3.4.2. Watermark Extraction Process

Assuming a video of the watermarked, the candidate co-efficient can be attained by conducting SVD decomposition afterwards DTCWT. Based on the following equation, the binary bit embedded in the frames is extracted.

$$w = \begin{cases}-1_t\ if\ SV_2^{i,k} < SV_4^{i,k} and SV_3^{i,k} < SV_5^{i,k}\\ 1, otherwise\end{cases} \tag{16}$$

Next, based on the length of the video, the extracted binary sequence was grouped into group-level watermarks. $flag = \sum_{i=1}^{i=c} w_i$ denotes standard for group-level watermark generation. Lastly, according to (17), the group-level watermark can be generated.

$$watermark_j = \begin{cases}1, & if\ flag > 0\\ -1, & if\ flag < 0\\ 2, & otherwise\end{cases} \tag{17}$$

4. Results and Discussion

In this part, the experimenting validation of the ABC-DTCWT-SVD method is tested using five input test images and a watermark image. Figure 3 illustrates the sample images. Figure 4 visualizes the generated watermarked images attained by the ABC-DTCWT-SVD method on 25 iterations. The watermarked images revealed that the ABC-DTCWT-SVD method has effectually embedded the watermarks on different iterations.

Figure 5 visualizes the extracted watermarked images obtained by the ABC-DTCWT-SVD technique on 25 iterations. The extracted images show that the ABC-DTCWT-SVD technique has effectually extracted the watermark image on different iterations.

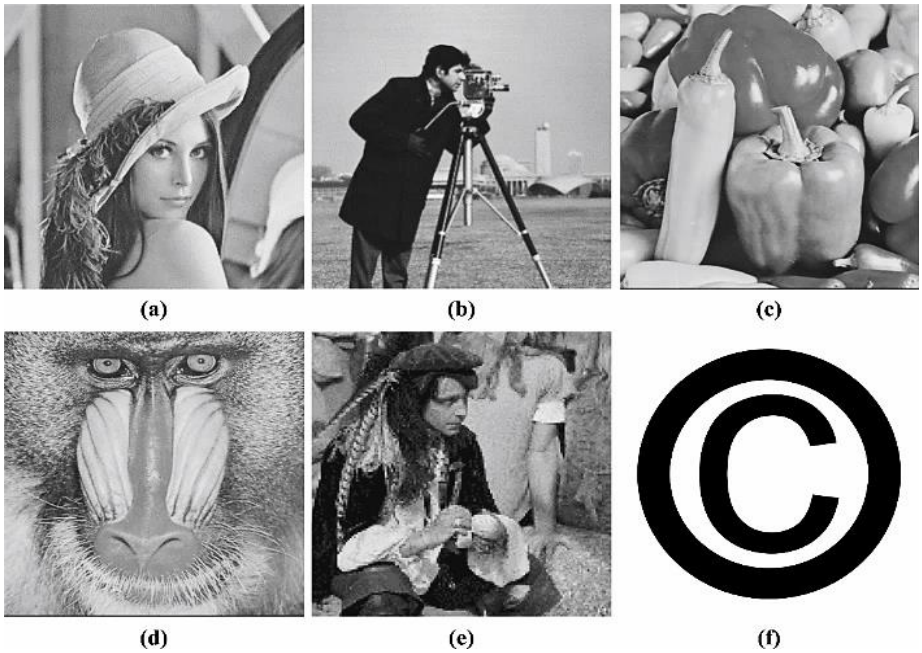

Fig. 3 Image instances (a-f) Lena, Cameraman, Peppers, Baboon, Man, and Secret image

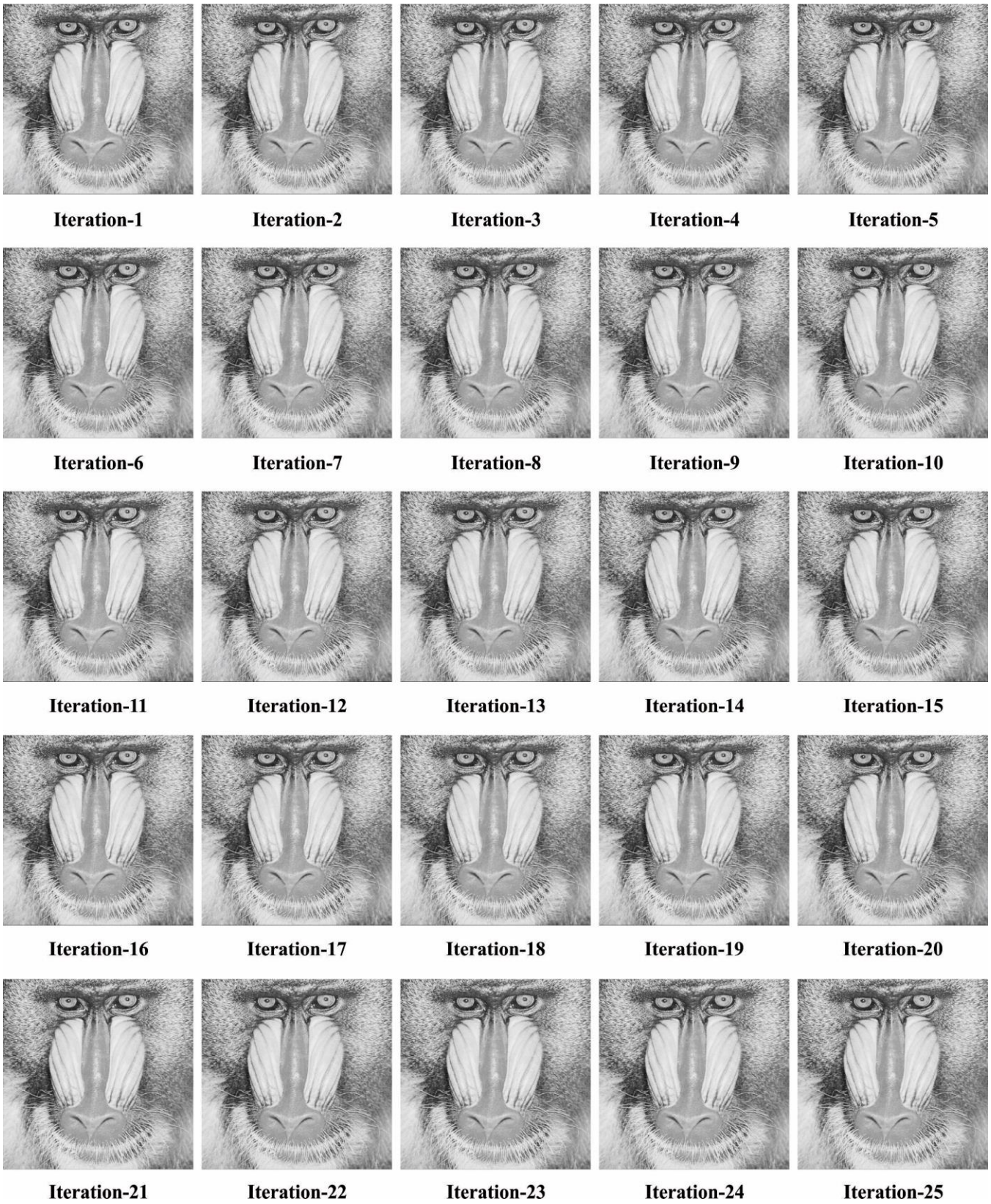

Fig. 4 Watermarked Images on 25 Iterations

Fig. 5 Extracted watermarked images on 25 iterations

Table 1. Sample of iterations on baboon image using several measures

Iterations	MSE	RMSE	PSNR	SSIM	NCC
1	3.4007	1.8441	42.8152	99.97	0.9998
2	1.617	1.2716	46.0438	99.98	0.9999
3	3.0959	1.7595	43.2229	99.97	0.9999
4	0.9833	0.9916	48.204	99.98	0.9999
5	3.0969	1.7598	43.2215	99.97	0.9999
6	0.0776	0.2786	59.2301	99.99	1.0000
7	3.4678	1.8622	42.7302	99.97	0.9998
8	1.6956	1.3022	45.8375	99.98	0.9999
9	0.601	0.7752	50.342	99.99	1.0000
10	0.6002	0.7748	50.3475	99.99	1.0000
11	2.7596	1.6612	43.7223	99.97	0.9999
12	0.9432	0.9712	48.3845	99.98	0.9999
13	0.1	0.3162	58.1305	99.99	1.0000
14	0.4659	0.6826	51.4475	99.99	1.0000
15	1.2637	1.1241	47.1145	99.98	0.9999
16	0.6122	0.7824	50.2619	99.99	1.0000
17	0.946	0.9726	48.372	99.98	0.9999
18	1.0256	1.0127	48.021	99.98	0.9999
19	2.8934	1.701	43.5167	99.97	0.9999
20	0.6279	0.7924	50.152	99.99	1.0000
21	3.1127	1.7643	43.1994	99.97	0.9999
22	0.4797	0.6926	51.3215	99.99	1.0000
23	1.6586	1.2879	45.9334	99.98	0.9999
24	1.9466	1.3952	45.2379	99.98	0.9999
25	1.6965	1.3025	45.8352	99.98	0.9999

Table 2. The average outcome of the ABC-DTCWT-SVD approach under various measures

Number of Images	MSE	RMSE	PSNR	SSIM	NCC
Image-1 (Lena)	0.065	0.254	60.023	100	1.00
Image-2 (Cameraman)	0.056	0.236	60.670	100	1.00
Image-3 (Peppers)	0.053	0.229	60.926	99.99	1.00
Image-4 (Baboon)	0.078	0.279	59.230	99.99	1.00
Image-5 (Man)	0.106	0.325	57.889	99.99	1.00

Table 1 demonstrates the overall watermarking results of the ABC-DTCWT-SVD technique obtained on the input baboon image. The results are taken for a set of 25 iterations. The results indicate that the ABC-DTCWT-SVD technique reaches higher PSNR, SSIM, and NCC values. At the same time, the ABC-DTCWT-SVD technique gains the least values of MSE and RMSE.

Figure 6 represents the watermarking results of the ABC-DTCWT-SVD technique under five different input images for a set of 25 iterations. The figure reveals that the ABC-DTCWT-SVD technique highlighted improved performance under all images and iterations.

Table 2 reports an average outcome investigation of the ABC-DTCWT-SVD approach on five images. The results demonstrate that the ABC-DTCWT-SVD technique reaches improved PSNR, SSIM, and NCC values.

Figure 7 demonstrates the MSE and RMSE investigation of the ABC-DTCWT-SVD technique. The results imply that the technique exhibits an effectual outcome with minimal MSE and RMSE values. In the 1st image, this technique achieves an MSE of 0.065 and an RMSE of 0.254. Meanwhile, in the 3rd image, the method attains an MSE of 0.053 and RMSE of 0.229. Moreover, in the 5th image, the ABC-DTCWT-SVD model gains an MSE of 0.106 and RMSE of 0.325.

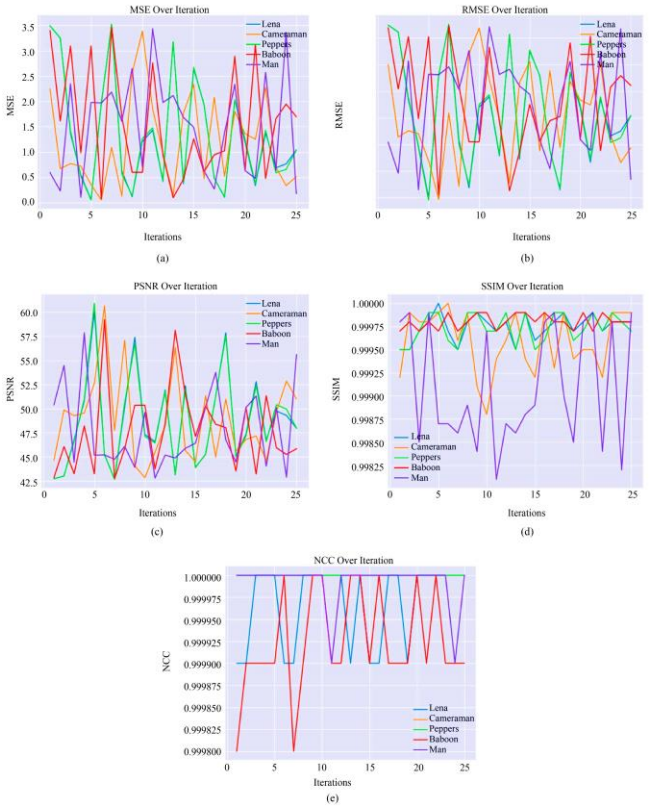

Fig. 6 Classifier outcome of ABC-DTCWT-SVD system (a) MSE, (b) RMSE, (c) PSNR, (d) SSIM, and (e) NCC

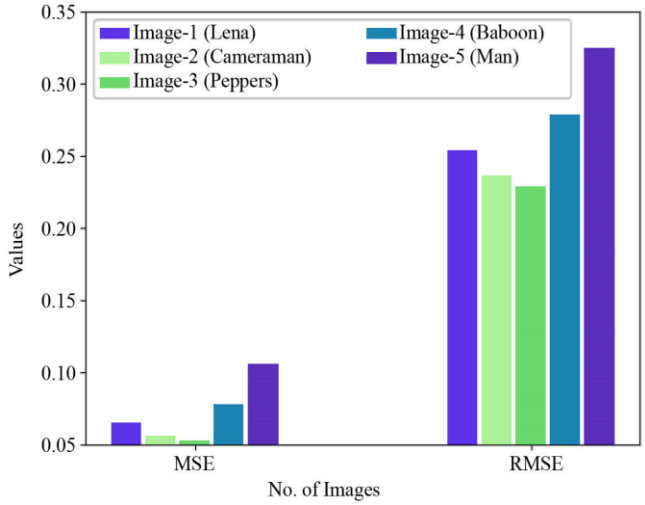

Fig. 7 MSE and RMSE outcome of ABC-DTCWT-SVD approach

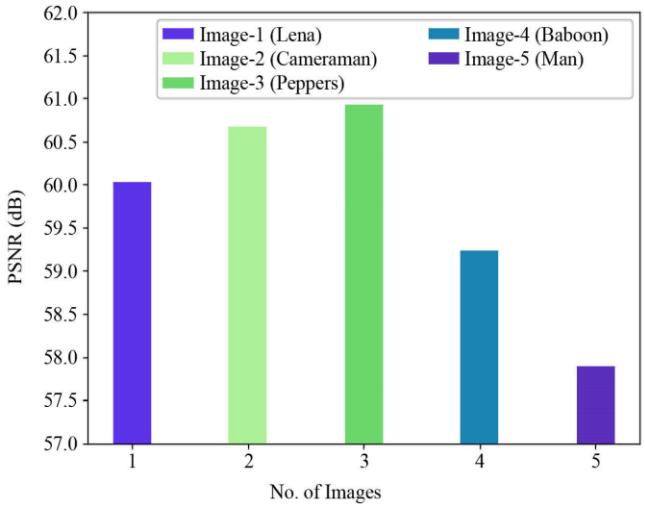

Fig. 8 PSNR outcome of ABC-DTCWT-SVD approach

The PSNR study of the ABC-DTCWT-SVD technique on different images is given in Figure 8.

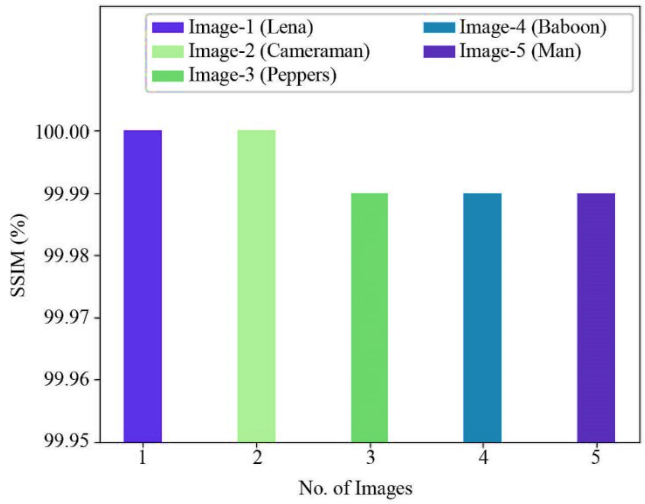

Fig. 9 SSIM outcome of ABC-DTCWT-SVD approach

The figure highlights the maximum outcomes of the ABC-DTCWT-SVD method with higher PSNR values under total imageries. For instance, in 1st image, the ABC-DTCWT-SVD technique attains a PSNR of 60.023dB. Next, in image 3, the ABC-DTCWT-SVD method attains a PSNR of 60.926dB. Then, in image 5, the ABC-DTCWT-SVD approach reaches a PSNR of 57.889dB.

The SSIM study of the ABC-DTCWT-SVD method on different images is introduced in Figure 9. The figure accentuates the maximum outcomes of the ABC-DTCWT-SVD system with higher SSIM values under total imageries. For instance, in 1st image, the ABC-DTCWT-SVD technique attains an SSIM of 100%. Next, in image 3, the ABC-DTCWT-SVD algorithm attains an SSIM of 99.99%. Then, in image 5, the ABC-DTCWT-SVD method attains an SSIM of 99.99%.

In Table 3 and Figure 10, a comparative PSNR inspection of the ABC-DTCWT-SVD method is performed [21].

Table 3. Comparative PSNR evaluation of ABC-DTCWT-SVD approach with other techniques

PSNR (dB)					
Methods	**1st Imagery**	**2nd Imagery**	**3rd Imagery**	**4th Imagery**	**5th Imagery**
ABC_DTCWT_SVD	60.023	60.670	60.926	59.230	57.889
SWT_MGWO	56.732	58.354	57.127	56.577	56.428
CSO_DIW	53.821	53.231	55.201	52.926	52.440
FA_DIW	50.757	51.574	53.555	55.370	51.093
MOAC_DIW	52.849	54.480	48.992	48.178	50.741
PSO_DIW	44.662	50.349	49.290	48.665	51.030

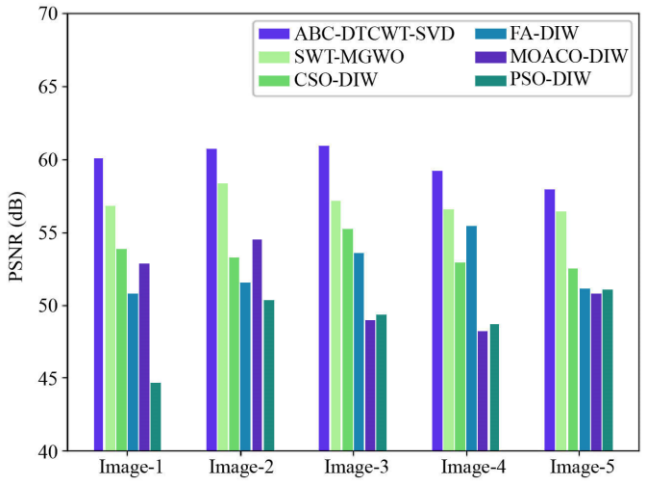

Fig. 10 PSNR investigation of ABC-DTCWT-SVD approach with other techniques

The experimental values highlighted that the ABC-DTCWT-SVD technique reaches higher PSNR values on all images. For instance, on image-1, the ABC-DTCWT-SVD technique gains increasing PSNR of 60.023dB while the MOACO_DIW, SWT_MGWO, FA_DIW, CSO_DIW, and PSO_DIW models obtain decreasing PSNR of dB: 56.732, 53.821, 50.757, 52.849, and 44.662 subsequently. Along with that, on image-3, the ABC-DTCWT-SVD method gains increasing PSNR of 60.926dB while the MOACO_DIW, SWT_MGWO, FA_DIW, CSO_DIW, and PSO_DIW methods obtain decreasing PSNR of dB: 57.127, 55.201, 53.555, 48.992, and 49.290 correspondingly. Finally, on image-5, the ABC-DTCWT-SVD algorithm gains increasing PSNR of 57.889dB while the MOACO_DIW, SWT_MGWO, FA_DIW, CSO_DIW, and PSO_DIW approaches gain decreasing PSNR of dB: 56.428, 52.440, 51.093, 50.741, and 51.030 subsequently.

The experimental outcomes confirmed the improved performance of the ABC-DTCWT-SVD technique over other existing models in the DIW process.

5. Conclusion

This study has introduced a new ABC-DTCWT-SVD approach for DIW. The primary objective of the ABC-DTCWT-SVD technique is to develop an image watermarking system to satisfy the requirements of imperceptibility and robustness.

In the ABC-DTCWT-SVD technique, the watermarking is embedded in the singular value of the cover imageries' DWT subbands. The watermarking will not be embedded straightaway on the wavelet co-efficient but rather on the element of the singular value of the cover imageries' DWT subbands. In addition, the ABC algorithm is used for the SVD approach's parameter tuning, thereby maximizing the PSNR values. The experimental result analysis of the ABC-DTCWT-SVD technique stated its promising performance over other techniques. In future, an encryption process can be included to increase the security of the watermark images.

References

[1] Lalita Verma, and Sanjay Pratap Singh Chauhan, "A Review on Digital Image Watermarking using Transformation and Optimization Techniques," *2nd International Conference on Advances in Computing, Communication Control and Networking (ICACCCN), IEEE*, pp. 1008-1012, 2020. [CrossRef] [Google Scholar] [Publisher Link]

[2] Mohammad Keivani et al., "Application of Empirical Wavelet Transform in Digital Image Watermarking," *Traitement du Signal*, vol. 37, no. 5, pp. 839-8445, 2020. [CrossRef] [Google Scholar] [Publisher Link]

[3] Xiaobing Kang et al., "Multi-Dimensional Particle Swarm Optimization for Robust Blind Image Watermarking using Intertwining Logistic Map and Hybrid Domain," *Soft Computing*, vol. 24, no. 14, pp. 10561-10584, 2020. [CrossRef] [Google Scholar] [Publisher Link]

[4] Ashwani Kumar, "A Review on Implementation of Digital Image Watermarking Techniques Using LSB and DWT," *Information and Communication Technology for Sustainable Development*, pp. 595-602, 2020. [CrossRef] [Google Scholar] [Publisher Link]

[5] R. Parthiban, and S. Manikandan, "Coyote Optimization Algorithm with Hybrid SVD-EVD Approach for Digital Image Watermarking," *SSRG International Journal of Electronics and Communication Engineering*, vol. 10, no. 5, pp. 49-61, 2023. [CrossRef] [Publisher Link]

[6] Dayanand G. Savakar, and Anand Ghuli, "Robust Invisible Digital Image Watermarking Using Hybrid Scheme," *Arabian Journal for Science and Engineering*, vol. 44, no. 4, pp. 3995-4008, 2019. [CrossRef] [Google Scholar] [Publisher Link]

[7] Manish Rai, and Sachin Goyal, "A Hybrid Digital Image Watermarking Technique based on Fuzzy-BPNN and Shark Smell Optimization," *Multimedia Tools and Applications*, vol. 81, pp. 39471-39489, 2022. [CrossRef] [Google Scholar] [Publisher Link]

[8] Rajkumar Ramasamy, and Vasuki Arumugam, "Robust Image Watermarking using Fractional Krawtchouk Transform with Optimization," *Journal of Ambient Intelligence and Humanized Computing*, vol. 12, no. 7, pp. 7121-7132, 2021. [CrossRef] [Google Scholar] [Publisher Link]

[9] Einolah Hatami et al., "An Optimized Robust and Invisible Digital Image Watermarking Scheme in Contourlet Domain for Protecting Rightful Ownership," *Multimedia Tools and Applications*, vol. 82, pp. 2021-2051, 2023. [CrossRef] [Google Scholar] [Publisher Link]

[10] Ch. Ravi Kumar, and P. Rajesh Kumar, "A Novel Semi-Blind Digital Image Watermarking using Fire Fly Algorithm," *Evolution in Signal Processing and Telecommunication Networks*, Springer, Singapore, vol. 839, pp. 463-473, 2022. [CrossRef] [Google Scholar] [Publisher Link]

[11] El-Sayed M. El-Kenawy et al., "Advanced Dipper-Throated Meta-Heuristic Optimization Algorithm for Digital Image Watermarking," *Applied Sciences*, vol. 12, no. 20, p. 10642, 2022. [CrossRef] [Google Scholar] [Publisher Link]

[12] Shiva Sattarpour, "Robust Optimal Image Watermarking using Graph-Based and Discrete Wavelet Transforms, and Whale Optimization Algorithm," *Multimedia Tools and Applications*, vol. 82, pp. 6667-6685, 2023. [CrossRef] [Google Scholar] [Publisher Link]

[13] Nilesh Dubey, and Hardik Modi, "A State of Art Comparison of Robust Digital Watermarking Approaches for Multimedia Content (Image and Video) Against Multimedia Device Attacks," *International Journal of Engineering Trends and Technology*, vol. 70, no. 8, pp. 132-139, 2022. [CrossRef] [Google Scholar] [Publisher Link]

[14] Payal Koolwal, and Sudhir Sharma, "Performance Improvement of Optimization Algorithm for Digital Image Watermarking in Hybrid DWT-DCT Transform," *International Conference on Electronics and Renewable Systems, IEEE*, pp. 1001-1005, 2022. [CrossRef] [Google Scholar] [Publisher Link]

[15] R. Radha Kumari, V. Vijaya Kumar, and K. Rama Naidu, "Optimized DWT based Digital Image Watermarking and Extraction Using RNN-LSTM," *International Journal of Interactive Multimedia and Artificial Intelligence*, vol. 7, no. 2, 2021. [CrossRef] [Google Scholar] [Publisher Link]

[16] Mokhtar Hussein, and B. Manjula, "A Hybrid Approach for SVD and Neural Networks Based Robust Image Watermarking," *International Journal of P2P Network Trends and Technology*, vol. 8, no. 4, pp. 1-5, 2018. [Publisher Link]

[17] Mohan Laavanya, and Marappan Karthikeyan, "Dual Tree Complex Wavelet Transform Incorporating SVD and Bilateral Filter for Image Denoising," *International Journal of Biomedical Engineering and Technology*, vol. 26, no. 3-4, pp. 266-278, 2018. [CrossRef] [Google Scholar] [Publisher Link]

[18] Arun Kumar R, Sai Kumar, and T. Venkat Narayana Rao, "Digital Image Watermarking Basedon Genetic Algorithm Approach," *International Journal of Computer & Organization Trends*, vol. 6, no. 6, pp. 34-37, 2016. [Publisher Link]

[19] Ebubekir Kaya, "A New Neural Network Training Algorithm based on Artificial Bee Colony Algorithm for Nonlinear System Identification," *Mathematics*, vol. 10, no. 19, p. 3487, 2022. [CrossRef] [Google Scholar] [Publisher Link]

[20] Yifei Wang et al., "A DTCWT-SVD based Video Watermarking Resistant to Frame Rate Conversion," *International Conference on Culture-Oriented Science and Technology, IEEE*, pp. 36-40, 2022. [CrossRef] [Google Scholar] [Publisher Link]

[21] Snehlata Maloo, Mahendra Kumar, and N. Lakshmi, "A Modified Whale Optimization Algorithm based Digital Image Watermarking Approach," *Sensing and Imaging*, vol. 21, 2020. [CrossRef] [Google Scholar] [Publisher Link]

[22] SonileKatungula Musonda, and John Soraghan, "Digital Image Watermarking in the Discrete Wavelet Domain and Analysis of the Effects of Compression on Watermarked Images," *SSRG International Journal of Electrical and Electronics Engineering*, vol. 2, no. 12, pp. 1-14, 2015. [CrossRef] [Publisher Link]

[23] K. Sakthidasan Sankaran et al., "Image Water Marking using DWT to Encapsulate Data in Medical Image," *International Conference on Communication and Signal Processing, IEEE*, pp. 0568-0571, 2019. [CrossRef] [Google Scholar] [Publisher Link]

[24] Kilari Jyothsna Devi et al., "A New Robust and Secure 3-Level Digital Image Watermarking Method Based on G-BAT Hybrid Optimization," *Mathematics*, vol. 10, no. 16, p. 3015, 2022. [CrossRef] [Google Scholar] [Publisher Link]

[25] Ali Pourhadi, and Homayoun Mahdavi-Nasab, "A Robust Digital Image Watermarking Scheme based on Bat Algorithm Optimization and SURF Detector in SWT Domain," *Multimedia Tools and Applications*, vol. 79, no. 29-30, pp. 21653-21677, 2020. [CrossRef] [Google Scholar] [Publisher Link]